# Connexin43 and connexin26 form gap junctions, but not heteromeric channels in co-expressing cells

**Joanna Gemel[1,*], Virginijus Valiunas[2,*], Peter R. Brink[2] and Eric C. Beyer[1,‡]**

[1]Department of Pediatrics, Section of Hematology/Oncology and Stem Cell Transplantation, University of Chicago, Chicago, IL 60637-1470, USA
[2]Department of Physiology and Biophysics, State University of New York at Stony Brook, Stony Brook, NY 11794, USA

*These authors contributed equally to this work
‡Author for correspondence (e-mail: ebeyer@peds.bsd.uchicago.edu)

*Accepted 6 January 2004*
*Journal of Cell Science 117, 2469-2480 Published by The Company of Biologists 2004*
*doi:10.1242/jcs.01084*

## Summary

**Many cells contain two (or more) gap junction proteins that are able to oligomerize with each other to form heteromeric gap junction channels and influence the properties of intercellular communication. Cx26 and Cx43 are found together in a number of cell types, but previous data have suggested that they might not form heteromeric connexons. We studied the possible interactions of these connexins by co-expression in three different cell lines. Analysis of N2aCx26/Cx43 cell pairs by double whole-cell patch-clamp methods showed that these cells were coupled, but contained only a small number of sizes of single channels consistent with those formed by homomeric Cx26 or Cx43 channels. Immunofluorescence studies showed that both connexins localized to appositional membranes, but in largely distinct domains. Analysis of Triton X-100-solubilized connexons from co-expressing cells by centrifugation through sucrose gradients or by affinity purification using a Ni-NTA column showed no evidence of mixing of Cx26 and Cx43. These results contrast with our observations in cells co-expressing other connexins with Cx43 and suggest that Cx26 and Cx43 do not form heteromeric hemichannels. Moreover, the incorporation of Cx26 and Cx43 into oligomers and into the membrane were similarly affected by treatment of co-expressing cells with brefeldin A or nocodazole, suggesting that the lack of mixing is due to incompatibility of these connexins, not to differences in biosynthetic trafficking.**

Key words: Intercellular communication, Heteromeric channels, Gap junctions

## Introduction

Gap junction channels mediate direct cell-to-cell communication by allowing passage of small molecules under about 1000 Da. Each gap junction channel is formed from two hemichannels each containing six protein subunits or connexins. More than 20 different mammalian connexins have been identified (Willecke et al., 2002).

Many cells express more than one connexin, and gap junction channels can potentially contain more than one type of connexin. One kind of mixed channel (a heterotypic channel) is formed by the pairing of two hemichannels containing different connexins. The compatibility (or incompatibilty) of different connexins for the formation of heterotypic channels has been extensively investigated in *Xenopus* oocyte (Swenson et al., 1989; Werner et al., 1989; Barrio et al., 1991; White and Bruzzone, 1996) and transfected cell (Elfgang et al., 1995; Suchyna et al., 1999; Valiunas et al., 2000; Elenes et al., 2001) expression studies. A heteromeric channel may form by the mixing of multiple connexins within the same hemichannel. Biochemical and physiological studies have identified a number of combinations of co-expressed connexins that can make heteromeric channels, including Cx26-Cx32 (Stauffer, 1995; Bevans et al., 1998), Cx46-Cx50 (Jiang and Goodenough, 1996), Cx43-Cx37 (Brink et al., 1997), Cx43-Cx56 (Berthoud et al., 2001), Cx40-Cx43 (He et al., 1999; Valiunas et al., 2001), Cx43-Cx45 (Martinez et al., 2002) and Cx26-Cx30 (Ahmad et al., 2003).

In order to begin to elucidate the rules, mechanisms, or sequences that allow different connexins to mix to form heteromeric channels, we wanted to study a combination of connexins that did not mix with each other to form heteromeric connexons. Several lines of evidence suggested that Cx26 and Cx43 might be good candidates. These two connexins are found together in a number of tissues or organs such as mammary epithelium (Tomasetto et al., 1993), skin (Risek et al., 1994; Goliger and Paul, 1995), colchea (Kikuchi et al., 2000) and testes (Brehm et al., 2002). Indeed, in leptomeningeal cells (Spray et al., 1991), thyroid cells (Meda et al., 1993), epidermal cells (Risek et al., 1994), P19 embryonal carcinoma cells (Belliveau et al., 1997), hypothalamic neuronal cell lines (Charles et al., 1996), lung epithelial cells (Lee et al., 1997) and astrocytes (Nagy et al., 2001), Cx26 and Cx43 are present in the same cells. Both connexins localize to appositional membranes in co-expressing cells. Yet, cell biological studies from a number of laboratories have suggested that they might not mix. For example, Spray et al. (Spray et al., 1991) found that Cx26 and Cx43 localize to discrete positions at appositional membranes in cultured leptomeningeal cells and make identifiable channels of discrete sizes. Risek et al. (Risek et al., 1994) identified very large gap junctions in epidermal cells that contained discrete domains of Cx26 or Cx43 immunoreactivity. Heterotypic pairing of Cx26 and Cx43 did not result in electrical coupling in paired *Xenopus* oocytes (White et al., 1995) nor did it allow dye

transfer in paired transfected HeLa cells (Elfgang et al., 1995) or mammary tumor cells (Tomasetto et al., 1993).

In the current studies, we expressed Cx43 and Cx26 together in stably transfected cells (N2aCx26/Cx43, HeLaCx26/Cx43(His)$_6$ and HEKCx26) and compared their behavior with cells expressing the individual connexins alone.

## Materials and Methods

### Cell culture

N2a cells were grown in Dulbecco's modified Eagle medium (DMEM) supplemented with 10% fetal bovine serum, 0.1 mM non-essential amino acids, 2 mM L-glutamine, 100 U/ml penicillin and 100 μg/ml streptomycin (Gibco-BRL). HeLa cells were grown in minimal essential medium supplemented with 10% fetal bovine serum, 0.1 mM non-essential amino acids, 2 mM L-glutamine, 100 U/ml penicillin and 100 μg/ml streptomycin (Gibco-BRL). HEK293 cells were grown in DMEM supplemented with 10% calf serum, 2 mM L-glutamine, 100 U/ml penicillin and 100 μg/ml streptomycin (Gibco-BRL).

Rat Cx26 or Cx43 DNAs were subcloned into eukaryotic expression plasmids (pcDNA3.1/neo or hygro). A construct containing a (His)$_6$ tag on the Cx43 C terminus and a construct containing an HA tag on the Cx26 C terminus were produced using PCR methods. While others have suggested that GFP may alter the ability of Cx43 to from large plaques in HeLa cells (Hunter et al., 2003), our previous studies have indicated no significant differences in the cell biological or physiological properties of Cx43(His)$_6$ from wild-type Cx43 when expressed in stably transfected HeLa cells (Martinez et al., 2002).

Cells were stably transfected with linearized DNA using lipofectamine (Gibco-BRL). Stable clones were selected by culturing in medium containing G418 (500 μg/ml) (Gibco-BRL) and/or hygromycin (150 μg/ml) (Calbiochem). Production of N2aCx43, N2aCx26, HeLaCx43(His)$_6$, HeLa-Cx40/Cx43 and HeLaCx45 cells have been described previously (Veenstra et al., 1992; Suchyna et al., 1999; Valiunas et al., 2001; Martinez et al., 2002). Cells that stably expressed both Cx26 and Cx43 were generated by transfection of N2aCx26 cells with Cx43(His)$_6$, HeLaCx43(His)$_6$ with Cx26 or HEK (which endogenously contain Cx43 protein and channels) with Cx26HA. Clones were screened for Cx26 or Cx43 expression by immunoblotting with anti-connexin antibodies.

### Cell treatments

HelaCx43/Cx26 or HEKCx26 cells were treated with 5 μg/ml brefeldin A or ethanol (used as the solvent) for 4 hours or 20 hours. The same cell lines were treated with 7.5 μg/ml nocodazole or DMSO (nocodazole solvent) for 4 hours or 20 hours.

### Solubilization of connexins and connexons with Triton X-100

Protein extraction was performed as described earlier (Berthoud et al., 2001). Briefly, cultured cells were harvested in incubation buffer (PBS containing 0.8 mM $MgSO_4$, 2.7 mM $CaCl_2$, 1 mM $Na_2V_2O_5$, 10 mM NaF, 10 mM N-ethylmaleimide, 20 mM N-2-Hydroxyethylpiperazine-N′-2-ethanesulfonic acid (Hepes) pH 7.5, 3 μg/ml antipain, 3 μg/ml phosphoromidon, 0.5 μg/ml aprotinin, 0.5 μg/ml leupeptin, 20 μg/ml Pefablock; protease inhibitors were purchased from Roche Molecular Biochemicals, Indianapolis, IN, USA) and centrifuged at 150 $\boldsymbol{g}$ for 7 minutes. Pelleted cells were resuspended in incubation buffer and extracted on ice for 30 minutes with 1% Triton X-100. Samples were centrifuged at 100,000 $\boldsymbol{g}_{ave}$ for 30 minutes and the supernatant containing solubilized connexons was used for experiments (immunoblot analysis, sedimentation through sucrose density gradients or purification of His-tagged proteins).

### Immunoblot analysis

Protein extracts from N2a cells were prepared as described previously (Laing and Beyer, 1995). Protein extracts from HeLa and HEK cells were prepared by Triton X-100 extraction as described above. Protein concentration was determined using the BioRad protein assay based on the Bradford dye-binding procedure (Bradford, 1976). Aliquots containing 20-100 μg of protein were separated by SDS-PAGE on 12% polyacrylamide gels and blotted onto Immobilon-P (Millipore). Immunoblots were developed with ECL chemiluminescence reagents (Amersham Pharmacia Biotech.). Peroxidase-conjugated goat anti-rabbit IgG (1:5000 dilution) or donkey anti-mouse IgG (1:4000 dilution) (Jackson ImmunoResearch Laboratories, Inc.) were used as secondary antibodies. Rainbow molecular mass marker standards (Amersham Pharmacia Biotech.) were used to calibrate the gels.

### Anti-connexin antibodies

Cx43 was detected using a mouse monoclonal antibody directed against amino acids 252-270 (Chemicon, mAb 3068), at 1:2000 dilution for immunoblots and 1:250 for immunofluorescence, or rabbit polyclonal antibodies directed against a bacterially expressed GST-Cx43 C-terminal fusion protein, at 1:20,000 dilution for blots and 1:2000 for immunofluorescence, or directed against amino acids 363-382 of Cx42 (Sigma Chemical Company, St Louis, MO, C6219), at 1:4000. Cx26 was detected using a mouse monoclonal antibody directed against a segment of the cytoplasmic loop of rat Cx26 (Zymed, 13-8100; at 1:500 dilution). Rabbit polyclonal antibodies directed against a synthetic peptide immunogen corresponding to residues 316-329 of dog Cx40 were affinity purified as described earlier (Kanter et al., 1993) and used at 1:250 dilution for immunofluorescence.

### Immunofluorescent labeling of cells

Cells cultured on multiwell slides were stained as described previously, except for the use of 4% paraformaldehyde for 30 minutes as a fixative. To increase the adherence of HEK cells, they were plated on slides coated for 30 minutes with a mixture of bovine collagen (Biomaterials) (30 μg/ml), human fibronectin (Chemicon) (10 μg/ml) and bovine serum albumin (Sigma Chemical Company St Louis, MO) (100 μg/ml) in PBS or with 0.01% poly L-lysine (Sigma Chemical Company, St Louis, MO). Cy3- (or Cy2-) conjugated goat anti-mouse or anti-rabbit IgG (Jackson ImmunoResearch Laboratories, Inc.) were used as secondary antibodies. For double-labeling experiments, cells were incubated simultaneously with both mouse anti-Cx43 monoclonal antibody and rabbit anti-HA antibodies (Zymed) (to detect tagged Cx26) or anti-Cx40 antibodies followed by Cy2- and Cy3-conjugated secondary reagents. For confocal microscopy, secondary antibodies Cy2 goat anti-rabbit IgG (1:100 dilution) and Alexa Fluor 660 goat anti-mouse IgG (1:500 dilution) (Molecular Probes) were used. Mouse monoclonal anti-Golgi 58K protein (clone 58K-9) and anti-β-tubulin antibodies were obtained from Sigma Chemical Company (St Louis, MO) and used at 1:1000 dilution.

Confocal images were obtained using an IX70 Olympus Fluoview 2000 laser-scanning confocal microscope (Melville, NY, USA) equipped with laser lines (488 nm, 543 nm and 633 nm). Images were collected by sequential scanning using single laser line-excitation to eliminate bleeding from one color channel into the other. Images were analyzed using Fluoview software.

### Affinity purification of His-tagged proteins

His-tagged proteins were purified using Ni-NTA resin (Qiagen) as described by the company in a protocol for batch purification under native conditions with several modifications. To reduce non-specific binding, the Ni-NTA resin was blocked for 15 minutes with 2.5% bovine serum albumin in lysis buffer. All buffers contained 1% Triton

X-100. Triton-extracted protein samples (prepared as described above) were incubated with resin for 2 hours at 4°C. The resin was washed extensively with buffer, and then bound proteins were eluted with a step gradient of L-histidine (1-200 mM). Samples were analyzed by immunoblotting.

### Sedimentation through sucrose density gradients

Velocity centrifugation of Triton X-100-solubilized material through sucrose gradients was performed as described by Berthoud et al. (Berthoud et al., 2001) as adapted from Musil and Goodenough (Musil and Goodenough, 1993) and Koval et al. (Koval et al., 1997). Samples were separated in a 5-20% linear sucrose gradient. In some cases, oligomers were dissociated by incubation of the Triton X-100-soluble material in 0.6% SDS for 1 hour at 4°C prior to layering on top of the sucrose gradient.

### Chemical cross-linking

Crosslinking of connexins in unfractionated HeLa or HEK cell lysates was performed as described by Musil and Goodenough (Musil and Goodenough, 1993). Cells were lysed in 1% Triton X-100 in PBS at 4°C and then centrifuged at 100,000 ***g*** for 30 minutes at 4°C. Supernatants containing connexons (hexamers) were diluted twofold with the lysis buffer and then reacted with 2 mM disuccinimidyl suberate (DSS; Pierce) or DMSO for 30 minutes. Samples containing 100 μg of protein were quenched with 50 mM Tris pH 7.5 for 15 min at 4°C and then run on 9% SDS-polyacrylamide gels and immunoblotted.

### Electrophysiological methods

Junctional currents from cell pairs were analyzed using the double whole-cell patch clamp technique as described previously (Brink et al., 1997; Valiunas et al., 2000; Valiunas et al., 2001).

During experiments, the cells were superfused with bath solution containing (in mmol/l): CsCl, 110; KCl, 5; $CaCl_2$, 2; $MgCl_2$, 1; HEPES, 10 (pH 7.4). The patch pipettes were filled with saline containing (mmol/l): CsCl, 110; $MgCl_2$, 0.1; $CaCl_2$, 0.1; EGTA, 3; HEPES, 10 (pH 7.2).

Glass coverslips with adherent cells were transferred to an experimental chamber perfused with bath solution at room temperature (21-23°C). The chamber was mounted on the stage of an inverted microscope (Olympus IMT2). Patch pipettes were pulled from glass capillaries (code 7052; A-M Systems) with a horizontal puller (Sutter lnstruments). When filled, the resistance of the pipettes measured 1-1.5 MΩ. Experiments were carried out on mixed cell pairs. Cell Tracker green (Molecular Probes) was always used in one of the two populations of cells to allow heterologous pairs to be identified (Valiunas et al., 2000). A dual voltage-clamp method and whole-cell recording were used to control the membrane potential ($V_m$) of both cells and to measure associated junctional currents ($I_j$) (Brink et al., 1996). Each cell was attached to a patch pipette connected to a separate micromanipulator (WR-88; Narishige Scientific Instrument). To measure $I_j$, both cells were held at the same holding potential, i.e. $V_h$=0 mV. The voltage of one of the cells ($V_1$ or $V_2$) was then stepped to different levels (Valiunas et al., 2000). A bipolar pulse protocol was used as described previously (Brink et al., 1997; Ramanan et al., 1999). The amplitudes of $I_j$ were determined at the beginning ($I_{j,inst;}$ *inst*: instananeous) and end of each pulse ($I_{j,ss}$; *ss*: steady state) to estimate the conductances $g_{j,inst}$ and $g_{j,ss}$, respectively (Valiunas et al., 2000; Valiunas et al., 2001). We have used $I_{j,ss}$ or $g_{jss}$ to indicate junctional current or conductance at the 10 second time points where $g_{jss}$ represents an approximation of the steady state. A number of step and ramp protocols were employed to assess single channel, multichannel and macroscopic junction conductance using the methods of Valiunas et al. (Valiunas et al., 2000). The duration of the ramps was 2 seconds and the peak amplitudes of the ramps were ±100 mV.

Voltage and current signals were recorded using patch clamp amplifiers (Axopatch 200). The current signals were digitized with a 16 bit A/D-converter (Digidata 1322A, Axon Instrument) and stored with a personal computer. Data acquisition and analysis were performed with custom-made software (Brink et al., 1996; Krisciukaitis, 1997) and pClamp8 software (Axon Instrument). Curve fitting and statistical analyses were performed using SigmaPlot and SigmaStat, respectively (Jandel Scientific). Unless otherwise noted, data were presented as mean values±s.e.m.

## Results

### Cx43 and Cx26 expression and localization in different transfectants

Stable cell lines co-expressing Cx43 and Cx26 were prepared by sequential transfection of communication-deficient cells (N2a or HeLa) with Cx43 and Cx26 or by transfection of HEK-293 cells (which endogenously express Cx43 protein and channels) with Cx26. We used multiple different cell lines (expressing either epitope-tagged or untagged connexins) to assure the generality of our conclusions and because of the relative advantages of certain cells for different analyses (N2a cells for electrophysiology; HeLa and HEK cells for biochemical and immunohistochemical analysis). Connexin expression was verified by immunoblotting (Fig. 1). All of the expected introduced connexins were identified. Moreover, introduction of a second connexin did not substantially alter the levels of the first connexin (i.e. compare Cx43 in HeLaCx43 and HeLaCx43/Cx26, Cx43 in HEK and HEKCx26, Cx26 in N2aCx26 and N2aC26/Cx43).

Immunofluorescent staining of the transfected cells showed that both Cx26 and Cx43 localized to appositional membranes in all of the transfectants. At relatively low magnification, many of the gap junction plaques in the co-expressing cells appeared to contain both connexins, as demonstrated by the coincidence of red and green staining of HEKCx26 cells in Fig. 2B,C and their superposition in Fig. 2A. However, some red and green spots appeared to be adjacent and non-overlapping or discrete (Fig. 2A-C). These observations were extended by confocal microscopy with simultaneous detection of Cx26 and Cx43 immunoreactivity. A stacked image produced from serial *Z*-sections through a large gap junction plaque showed substantial domains labeled only red or green as well as an area of yellow overlap (Fig. 2D). Individual confocal sections, viewed at relatively higher magnification, confirmed the presence of domains within gap junction plaques that were exclusively one color, indicating the detection of only one connexin (Fig. 2E-H). These observations contrasted strongly with similar analysis of large plaques in the cells that we have previously prepared which co-expressed Cx40 and Cx43 (Valiunas et al., 2001). The red and green colors were perfectly superimposed in confocal slices from HelaCx43/Cx40 cells, suggesting co-localization of Cx40 with Cx43 (Fig. 2I-K).

### Electrophysiological characterization of gap junction currents and channels in cells co-expressing Cx26 and Cx43

We analyzed the gap junctional currents in pairs of N2a cells co-transfected with Cx26 and Cx43 using the double whole cell

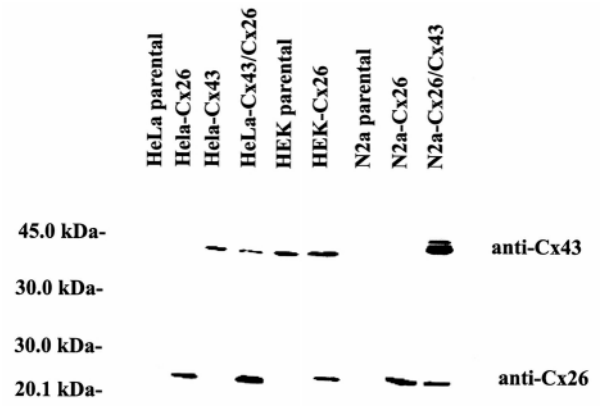


**Fig. 1.** Immunoblot detection of Cx43 and Cx26 expression in parental and stably transfected HeLa, HEK, and N2a cells. Triton X-100-soluble extracts prepared from HeLa cells (20 μg protein) or HEK cells (20 μg protein for Cx43 detection or 100 μg protein for Cx26 detection) or whole cell lysates prepared from N2a cells (75 μg protein) were resolved by SDS-PAGE, transferred to membranes and blotted with anti-Cx43 (top) or anti-Cx26 (bottom) antibodies. Migration of molecular mass markers is indicated to the left of the blot.

patch clamp technique. Most of these cell pairs (20/31) showed substantial intercellular coupling with a mean total junctional conductance ($g_j$) of 3.8 nS (Table 1). We obtained a similar frequency of coupled pairs and levels of macroscopic coupling when the co-expressing cells were paired with N2aCx26 or N2aCx43 cells. However, the $g_j$ observed for homotypic pairs of N2aCx26 or N2aCx43 cells was about eight times greater, and all of these cell pairs were coupled. Based on observed single channel conductances, it appeared that the co-expressing cell pairs had only 40-50 functional channels compared with 200-400 in the pairs of cells expressing only one connexin. Coupling in the co-expressing cells could not be explained by the formation of heterotypic Cx26-Cx43 channels, since only 25% of N2aCx26-N2a-Cx43 cell pairs examined showed any detectable coupling, and the mean $g_j$ was only 90 pS in these cell pairs. We also excluded a significant contribution of endogenous Cx45 in the N2a cells, since heterotypic Cx26-Cx45 coupling was similarly infrequent and poor.

The currents observed in pairs of N2aCx26/Cx43 cells showed a moderate time- and voltage-dependent decrease in amplitude (Fig. 3A). The steady-state conductances, $g_{j,ss}$, from multiple experiments could be fit to a Boltzman equation with parameters $V_{j,0}$=–97 mV/90 mV, $g_{j,min}$=0.3/ 0.4, $z$=1.4/1.1 for negative and positive $V_j$, respectively (Fig. 3B). The voltage-dependent behavior of the junctional currents in N2aCx26/Cx43 cells appeared somewhat intermediate between the behaviors of homotypic/homomeric Cx26 or Cx43 channels as demonstrated by recordings from N2aCx26-N2aCx26 or N2aCx43-N2aCx43 cell pairs or by pairing of a N2aCx26/Cx43 cell with and N2aCx26 cell (Fig. 3A, right panel). Moreover, in some cell pairs containing only relatively few channels, the currents very closely resembled those of pure Cx26 or Cx43 connexons.

In poorly coupled pairs of N2aCx26/Cx43 cells, individual channel events were observed (Fig. 4A, Fig. 5A). Only a few different sizes of single channels were observed. Event histograms of N2aCx26/Cx43 cells (Fig. 6, top right panel) showed that these cells primarily contained events of two sizes, ~70 pS and ~135 pS (as exemplified in Fig. 4A). These unitary channel events closely corresponded to the sizes of homotypic/homomeric Cx43 and Cx26 channels that we observed in pairs of N2aCx26 cells and N2aCx43 cells (Fig. 5B and Fig. 6) and that have been previously reported (Suchyna et al., 1999; Valiunas et al., 2000). The absence of additional channel types in the co-expressing cells was further verified by pairing co-expressing cells with N2a cells expressing only a single connexin. These studies yielded very similar histograms for N2aCx26/Cx43-N2aCx26 cell pairs compared with N2aCx26-N2aCx26 pairs, and for N2aCx26/Cx43-N2aCx43 cell pairs compared with N2aCx43-N2aCx43 pairs (Fig. 6). All cell pairs

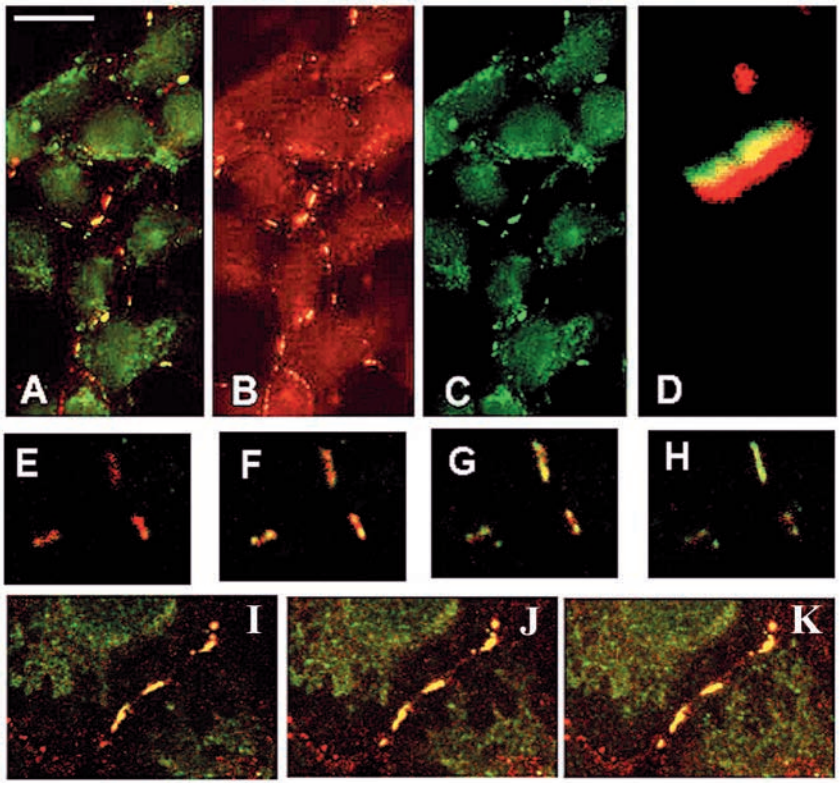


**Fig. 2.** Detection of the distributions of Cx26 (red) and Cx43 (green) in HEKCx26 cells (A-H) or Cx40 (red) and Cx43 (green) in HeLa-Cx43/Cx40 cells (I-K) by immunofluorescence microscopy. (A-C) Conventional immunofluorescence images of cells double labeled for Cx26 (shown alone in B) and for Cx43 (shown alone in C). Merged image of both immunoreactivities is shown in A. (D) Stacked z-series from double label confocal analysis of a single large plaque. (E-H) Z-series of slices obtained at different depths (separated by 0.3-1.2 μm) from confocal analysis of plaques in HEK-Cx26 cells. (I-K) Z-series of slices similarly obtained at different depths from plaques in pairs of HeLa-Cx43/Cx40 cells where simultaneously obtained images show precise co-localization of Cx43 (red) and Cx40 (green). Bar: 27 μm (A-C); 1 μm (D); 5 μm (E-H); 3 μm (I,J).

contained some small conductance events ≤30 pS) which may represent endogenous channels (probably Cx45).

The appearance of the single channel events in N2aCx26/Cx43-N2aCx26 cell pairs also closely resembled homotypic/homomeric Cx26 channels. The N2aCx26/Cx43-N2aCx43 cell pairs (Fig. 4B) exhibited Cx43-like channels with mainstate conductances ($\gamma_{j,ms}$) of 69-72 pS for positive and negative $V_j$, respectively, as well as a residual state ($\gamma_{j,res}$) of 16 pS-17pS, similar to the channels recorded from pairs of N2aCx43 cells. The N2aCx26/Cx43 cell pairs exhibited mainly two types of channels: the Cx26-like channels with $\gamma_{j,ms}$ of ~130-135 pS (Fig. 5A, middle panel) and channels with prominent rectification (94/130 pS, for positive and negative $V_j$, respectively (Fig. 5A, bottom panel) when recorded using a voltage ramp protocol. Very similar channel sizes and behavior were observed in homotypic N2aCx26 cell pairs (Fig. 5B). Indeed, rectifying channel currents from a co-transfected N2aCx26/Cx43 cell pair appeared superimposible with a channel from an N2aCx26-N2aCx26 cell pair, suggesting they are the same type of channel (Fig. 5C).

**Table 1. Electrophysiological data obtained from different types of N2A cell pairs**

| Cell pair type | Investigated cell pairs | Coupled cell pairs | Total conductance $g_j$ (nS) | Single-channel conductance $\gamma_{j,main}$ (pS) |
|---|---|---|---|---|
| Cx26/43-Cx26/43 | 31 | 20 | 3.8±1.1 | 25-153 |
| Cx26-Cx26 | 11 | 11 | 30.5±5.2 | 29-165 |
| Cx43-Cx43 | 9 | 9 | 29.0±3.5 | 29-84 |
| Cx26/43-Cx26 | 10 | 8 | 6.3±0.9 | 27-161 |
| Cx26/43-Cx43 | 11 | 7 | 3.3±1.5 | 27-82 |
| Cx26-Cx43 | 24 | 6 | 0.09±0.05 | 28-63 |
| Cx26-Cx45 | 23 | 9 | 0.06±0.01 | 27-37 |

Cell pairs consisting of different types of cells were examined for total gap junction conductance, $g_j$, and unitary conductance, $\gamma_{j,main}$. All connexins were expressed by the stable transfection of N2A cells, except for Cx45 which was expressed in HeLa cells. The numbers refer to mean values±s.e.m.

## Oligomerization of Cx26 and Cx43 in co-expressing cells

The possible association of Cx26 and Cx43 within oligomeric connexons was analyzed by velocity centrifugation or by affinity chromatography of detergent-solubilized material from co-expressing cells.

We and others have previously used sedimentation of a Triton-X100-soluble cellular fraction through sucrose density gradients to resolve monomeric and oligomeric connexin forms (Musil and Goodenough, 1993; Koval et al., 1997; Diez et al., 1999; Berthoud et al., 2001; Valiunas et al., 2001). We again used this technique to study the assembly of oligomeric connexin forms in HeLaCx43/Cx26 cells and compared our observations with the behavior of Cx26 or Cx43 in cells expressing only the individual connexins (Fig. 7). The gradients from HelaCx26 cells contained two peaks, one at 7.4% sucrose and the other at 13.4% sucrose; pretreatment of such samples with SDS, to disrupt oligomers, collapsed the Cx26 immunoreactive material to a single peak at 7.4% sucrose confirming that this peak

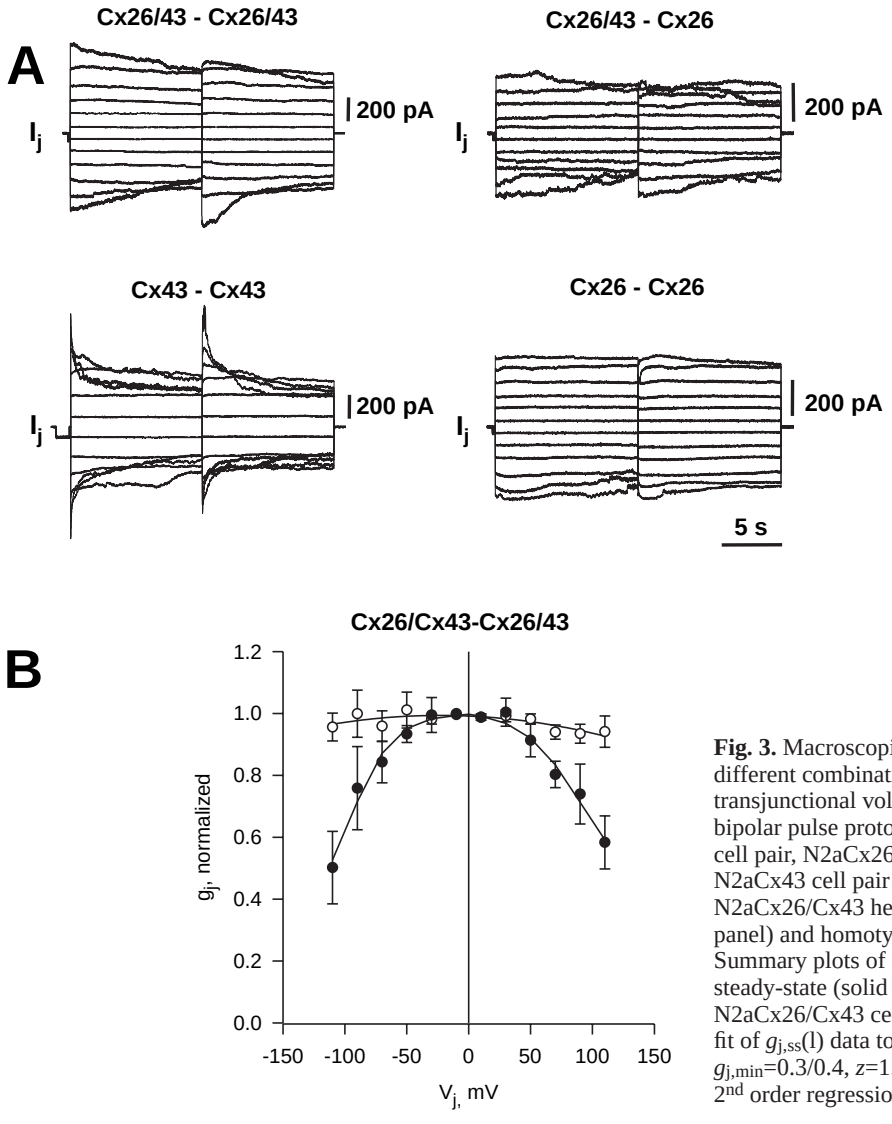


**Fig. 3.** Macroscopic currents recorded from N2a cell pairs containing different combinations of Cx26 and Cx43 and their dependence on transjunctional voltage ($V_j$). (A) Gap junction currents ($I_j$) elicited by bipolar pulse protocol from different N2A cell pairs: co-transfected cell pair, N2aCx26/Cx43-N2aCx26/Cx43 (top left panel); homotypic N2aCx43 cell pair (bottom left panel); co-transfected cell N2aCx26/Cx43 heterotypically paired with N2aCx26 cell (top right panel) and homotypic N2aCx26 cell pair (top right panel). (B) Summary plots of normalized instantaneous (open circles) and steady-state (solid circles) $g_j$ versus $V_j$ from 7 co-transfected N2aCx26/Cx43 cell pairs. The continuous curves represent the best fit of $g_{j,ss}$(l) data to the Boltzman equation ($V_{j,0}$=–97 mV/90 mV, $g_{j,min}$=0.3/0.4, $z$=1.4/1.1 for negative/positive $V_j$, respectively) and 2$^{nd}$ order regression ($r^2$=0.63) fit of $g_{j,ss}$ (O) data.

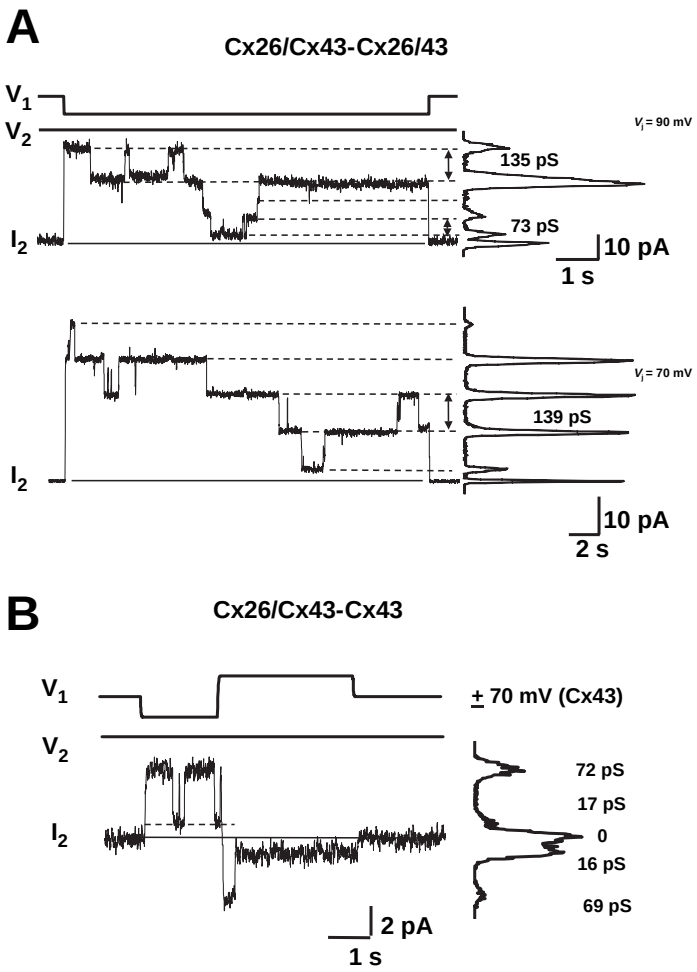


**Fig. 4.** Single channel properties of gap junctions recorded from co-transfected N2aCx26/Cx43 cells compared to those from a heterotypic N2aCx26/Cx43-N2aCx43 cell pair. (A) Single channel properties of events in pairs of co-transfected N2aCx26/Cx43 cells. (Top panel) Multichannel recording during maintained $V_j$ of 90 mV. Solid line represents zero current level; dashed lines represent discrete current steps indicative of opening and closing of channels. The current histograms indicate operation of at least two different channels with conductances of 135 pS and 73 pS (arrows) that resemble homotypic Cx26 and homotypic Cx43 channels, respectively. (Bottom panel) Multichannel recording during maintained $V_j$ of 70 mV. The current histograms revealed a conductance of 139 pS (resembling homotypic Cx26 channels). (B) Bipolar pulse protocol ($V_1$ and $V_2$) and associated single channel currents ($I_j$) recorded from a N2aCx26/Cx43-N2aCx43 cell pair. Current histograms yielded similar conductances for positive and negative $V_j$: 69 pS and 72 pS for the main state and 16 pS-17pS for the residual state (dashed line) (which correspond to homotypic Cx43 channels).

contained Cx26 monomers (Fig. 7A,B). The Cx26 oligomeric peak was detected in higher percentages of sucrose than expected, or than observed for Cx43 oligomers, but migrated consistently. Immunoreactive Cx43 from HeLaCx43 cells was detected in two peaks at 8.5% and 11% sucrose (Fig. 7C), which we have previously assigned to Cx43 monomers and oligomers, respectively (Berthoud et al., 2001; Valiunas et al., 2001). When Triton X-100-soluble material from the co-expressing HeLaCx43/Cx26 cells was similarly analyzed, the peaks of Cx26 and Cx43 immunoreactivity appeared in identical positions to the material from single connexin-expressing cells (Fig. 7D). The oligomeric peaks of Cx26 and Cx43 showed very little overlap suggesting that there were few connexons (or larger assemblies) that contained both connexins.

The potential association of Cx26 with Cx43 was also analyzed by affinity purification of Cx43 (containing a 6Xhistidine tag at the carboxyl terminus) from HeLa cells co-transfected with Cx26 and Cx43(His)$_6$ using a similar strategy to the one we used previously to show the association of Cx40 and Cx43 in co-expressing cells (Valiunas et al., 2001). The His-tag allowed the Cx43 to bind to the column and be specifically eluted, but because the Cx26 did not contain the tag any purified Cx26 must have been associated with Cx43. Connexons were solubilized with Triton X-100, and this material containing both immunoreactive Cx26 and Cx43 (Fig. 8, 'before column') was applied to a Ni/NTA affinity resin. The resin was extensively washed, and then eluted with increasing concentrations of histidine (Fig. 8). Little Cx43 was detected in the 'flow through' and a large amount of Cx43 was detected in the eluted material, indicating that all, or virtually all of it bound to the column. In contrast, Cx26 was detected only in the flow through and wash fractions, with no Cx26 detected in histidine-eluted fractions, suggesting that Cx43(His)-containing connexons did not contain Cx26.

### Is lack of interaction between Cx43 and Cx26 within hemichannel caused by different trafficking of these connexins?

A possible explanation for the lack of mixing of Cx26 and Cx43 within the same connexons (or even the same domains within gap junction plaques) is that they do not follow the same cellular routes for biosynthetic trafficking. It is generally believed that most connexins, including Cx43, travel through the Golgi apparatus and the classic secretory pathway similar to many plasma membrane and secreted proteins (Musil and Goodenough, 1993; George et al., 1999). In contrast, it has been proposed that Cx26 is directed through a shorter, alternative pathway, by-passing the Golgi apparatus (Evans et al., 1999). In these studies, these pathways were distinguished by their differential pharmacologic sensitivity to brefeldin A which disassembles the Golgi (but did not block Cx26 transport) and nocodazole, a microtubule disrupting reagent (which blocked Cx26) (George et al., 1999; Martin et al., 2001). However, these conclusions are controversial and not consistent with other published data (Thomas et al., 2001; Johnson et al., 2002). We tested these agents in our co-expressing cells.

We treated HEKCx26 cells or HeLaCx43/Cx26 cells for various times with brefeldin A or nocodazole and examined the location of the connexins or their state of oligomerization. Untreated HEKCx26 cells contained intense immunofluorescent staining for both Cx26 (Fig. 9A) and Cx43 (Fig. 9D) at appositional membranes. However, after 20 hours in brefeldin A, virtually all immunoreactive Cx26 (Fig. 9B) and Cx43 (Fig. 9E) had been lost from the membrane. The effectiveness of the brefeldin A treatment was confirmed by staining of cells with anti-Golgi 58K antibody (not shown). In

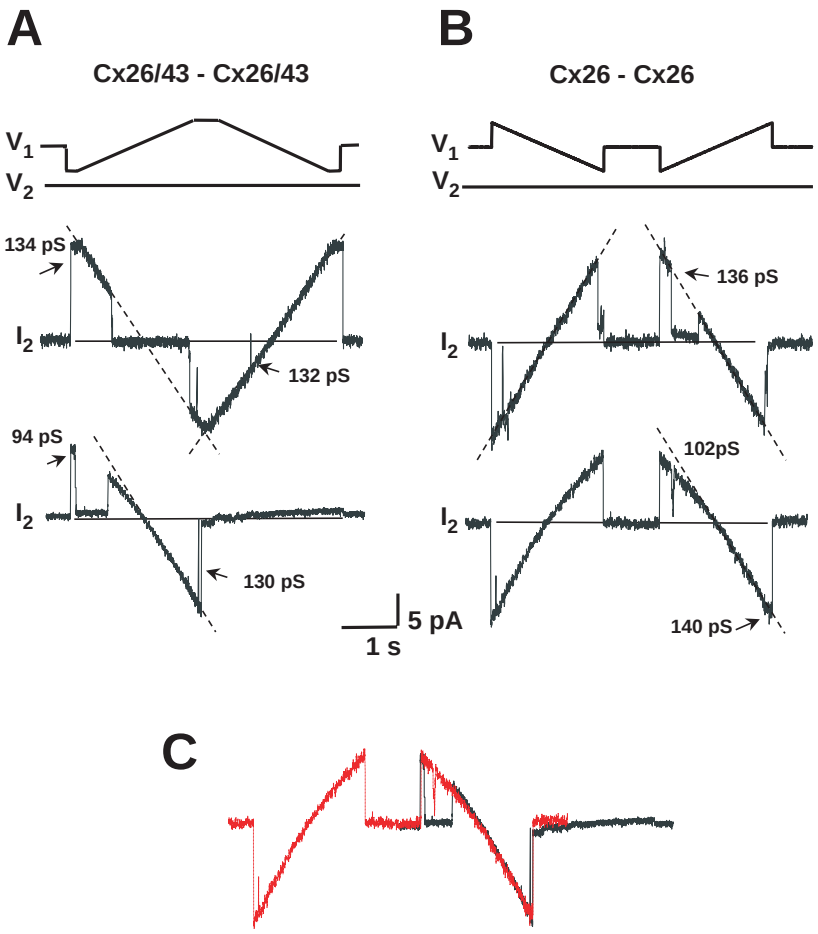


**Fig. 5.** Single channel properties of gap junctions recorded from co-transfected N2aCx26/Cx43 cells compared to homotypic Cx26 channels. (A) Single channel recordings from pairs of co-transfected N2aCx26/Cx43 cells. A voltage ramp protocol (top panel)$V_j$=±100 mV, ramp duration 2 seconds) evoked single channel currents (middle panel) with a slope conductance (dashed line) corresponding to a unitary conductance $g_j$ of 132-134 pS, which resembles homotypic Cx26 channels. The bottom panel shows another recording of one operational channel with channel rectification ($g_j$=94 pS at $V_j$=–100 mV and $g_j$=130 pS at $V_j$=100 mV). (B) Single channel recordings from pairs of homotypic N2aCx26 cells. (Middle panel) Single channel current elicited by voltage ramp protocol ($V_j$=±100 mV, 2 seconds) exhibited a unitary conductance, $g_j$ of 136 pS. (Bottom panel) Single channel currents of homotypic Cx26 showed rectification ($g_j$=102 pS at $V_j$=–100 mV and $g_j$=140 pS at $V_j$=100 mV). **(**C**)** Superposition of gap junction currents from a co-transfected N2aCx26/Cx43-N2aCx26/Cx43 pair and from a homotypic N2aCx26-N2aCx26 cell pair suggests that the same type of channel was recorded in both cases (i.e. Cx26).

contrast, nocodazole treatment for 20 hours produced little effect on the amount of Cx26 (Fig. 9C) or Cx43 (Fig. 9F) connexins seen at the appositional membranes. There was a significant change in the immunofluorescence of gap junction plaques after this drug treatment, probably because of the change in shape of these cells (rounding up). Immunofluorescent staining with anti-tubulin antibody confirmed total disruption of microtubules in these experimental conditions (not shown).

The effects of these agents on the oligomerization of Cx43 and Cx26 were tested by chemical cross-linking or velocity gradient centrifugation of Triton X-100-solubilized connexons from HeLaCx43/Cx26 cells. Connexons from untreated cells were reacted with crosslinker DSS or buffer alone; immunoblots of this material showed multiple bands in the cross-linked sample that migrated consistently with the positions expected for connexin monomers, dimers and higher oligomers (Fig. 10, time 0). Treatment of the cells with brefeldin A for progressive times led to disproportionate loss of the slower migrating bands. Treatment for 20 hours also led to a decrease in total Cx26 (by 76%) and Cx43 (by 25%) possibly due to an inhibition of protein synthesis by this drug in cultured cells (Fishman and Curran, 1992). Similar treatment of these cells with nocodazole had no effect on Cx26 or Cx43 oligomers as detected by chemical cross-linking (not shown). The effects of BFA on Cx26 connexin oligomerization were also studied in a sucrose gradient experiment. HelaCx43/Cx26 cells treated with brefeldin A for 20 hours only contained a single peak of Cx26 co-sedimenting with the monomer peak (not shown).

## Discussion

We have presented data showing that while Cx26 and Cx43 can be co-expressed in the same cells and participate in the formation of the same gap junction plaques, they do not form heteromeric connexons. Electrophysiological data show that co-expressing cells only contain channels with the characteristics of homotypic/homomeric Cx26 or Cx43 channels. Moreover, Cx26 was not isolated along with Cx43 when connexons were analyzed by centrifugation through sucrose gradients or by affinity chromatography. The lack of heteromeric mixing by Cx26 and Cx43 is consistent with the previous observations suggesting lack of precise co-localization of co-expressed Cx26 and Cx43 (Spray et al., 1991; Risek et al., 1994; Falk, 2000) and demonstrates their inability to form functional heterotypic channels in paired *Xenopus* oocytes (White et al., 1995) or to allow dye transfer in transfected cells (Elfgang et al., 1995).

Rectifying behavior of junctional currents has been used to identify some heterotypic gap junctions (Barrio et al., 1991; White and Bruzzone, 1996). We also noted rectification in cell pairs in which Cx26 and Cx43 were co-expressed (Fig. 5), but we also obtained single channel recordings where homotypic

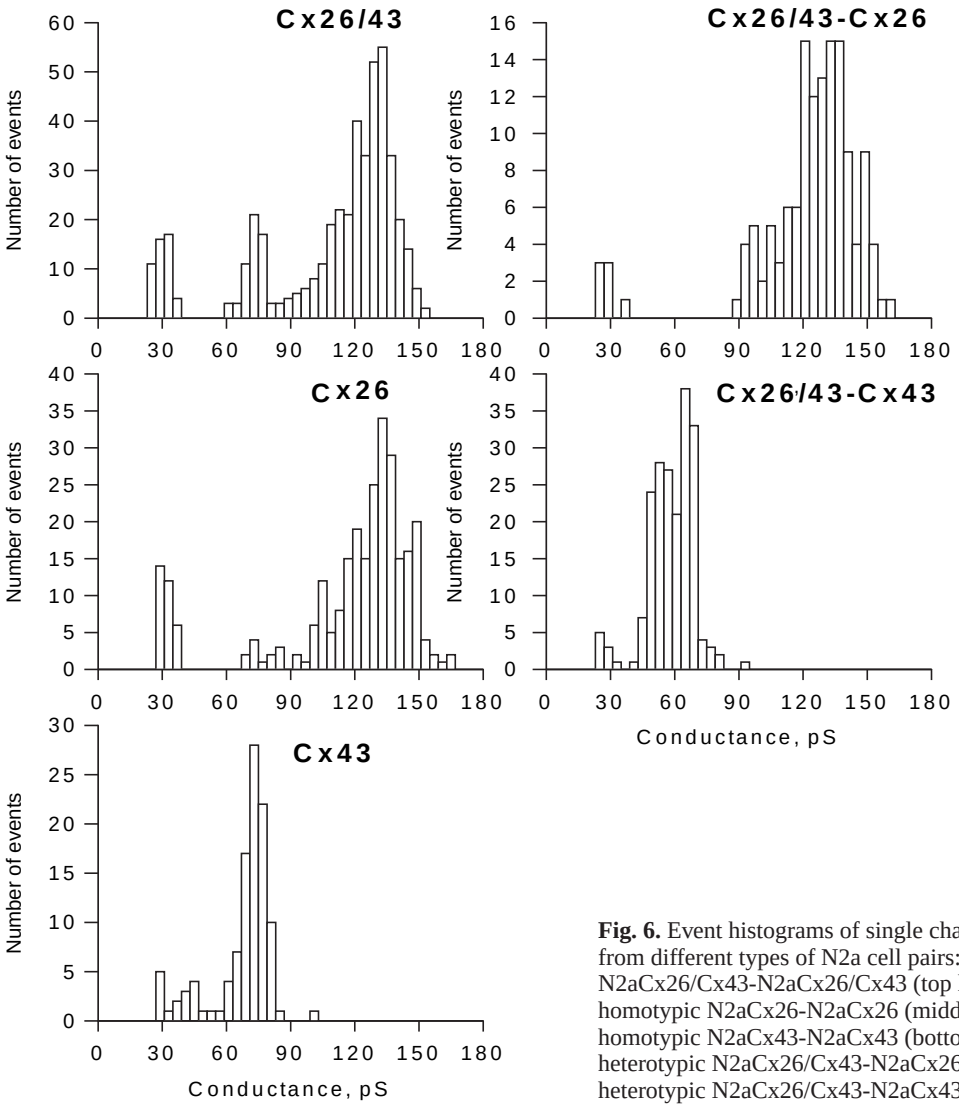


**Fig. 6.** Event histograms of single channel conductances from different types of N2a cell pairs: co-transfected N2aCx26/Cx43-N2aCx26/Cx43 (top left panel); homotypic N2aCx26-N2aCx26 (middle left panel); homotypic N2aCx43-N2aCx43 (bottom left panel); heterotypic N2aCx26/Cx43-N2aCx26 (top right panel) and heterotypic N2aCx26/Cx43-N2aCx43 (lower right panel).

Cx26 channels showed indistinguishable linear and rectifying I-V curves in response to ramp protocols. Previously published macroscopic records of homotypic Cx26 show voltage-dependent rectification that is similar to the rectification that we observed at the single channel level (Verselis et al., 1993). The simplest explanation for the rectification in both cases (macroscopic and single channel recordings) is a plasma membrane voltage dependence or inside-out voltage dependence reminiscent of some invertebrate gap junction channels (Verselis et al., 1991). It remains unknown why some channels rectify while others do not. Cx43 has not been shown to rectify in the manner of Cx26. Its I-V curve is linear. Regardless, the rectification provides no evidence for identifying heterotypic or heteromeric channels formed of Cx26 and Cx43.

Our data suggest that there is a cellular sorting mechanism that leads to different distributions of connexins in gap junction plaques. Our observations are very similar to those of Falk (Falk, 2000). He studied HeLa cells transfected with connexins tagged with the cyan and yellow variants of green fluorescent protein, and he observed that while both Cx43 and Cx26 could be identified at the same gap junction plaques, they were completely segregated into domains containing only one connexin isotype. Any apparent overlap of the proteins disappeared when deconvolution microscopy was used. He concluded that segregation of channels does not depend on plaque size nor on the ratio at which Cx26 and Cx43 are expressed.

What are the rules for heteromer formation? Connexins have been classified into major groups (termed α and β) based on their sequences (Kumar and Gilula, 1992). It has been proposed that connexins from one subgroup will only pair (or mix) with other members of the same subgroup (Yeager and Nicholson, 1996; Kumar, 1999). The ability of different connexins to form functional heterotypic channels roughly follows this classification, but with many exceptions (reviewed by Harris, 2001). The published data regarding functional heteromeric combinations are less extensive, but largely consistent. Functional heteromers are formed between combinations of α-connexins including Cx50 and Cx46 (Jiang and Goodenough, 1996), Cx43 and Cx37 (Brink et al., 1997), Cx43 and Cx56 (Berthoud et al., 2001) and Cx40 and Cx43

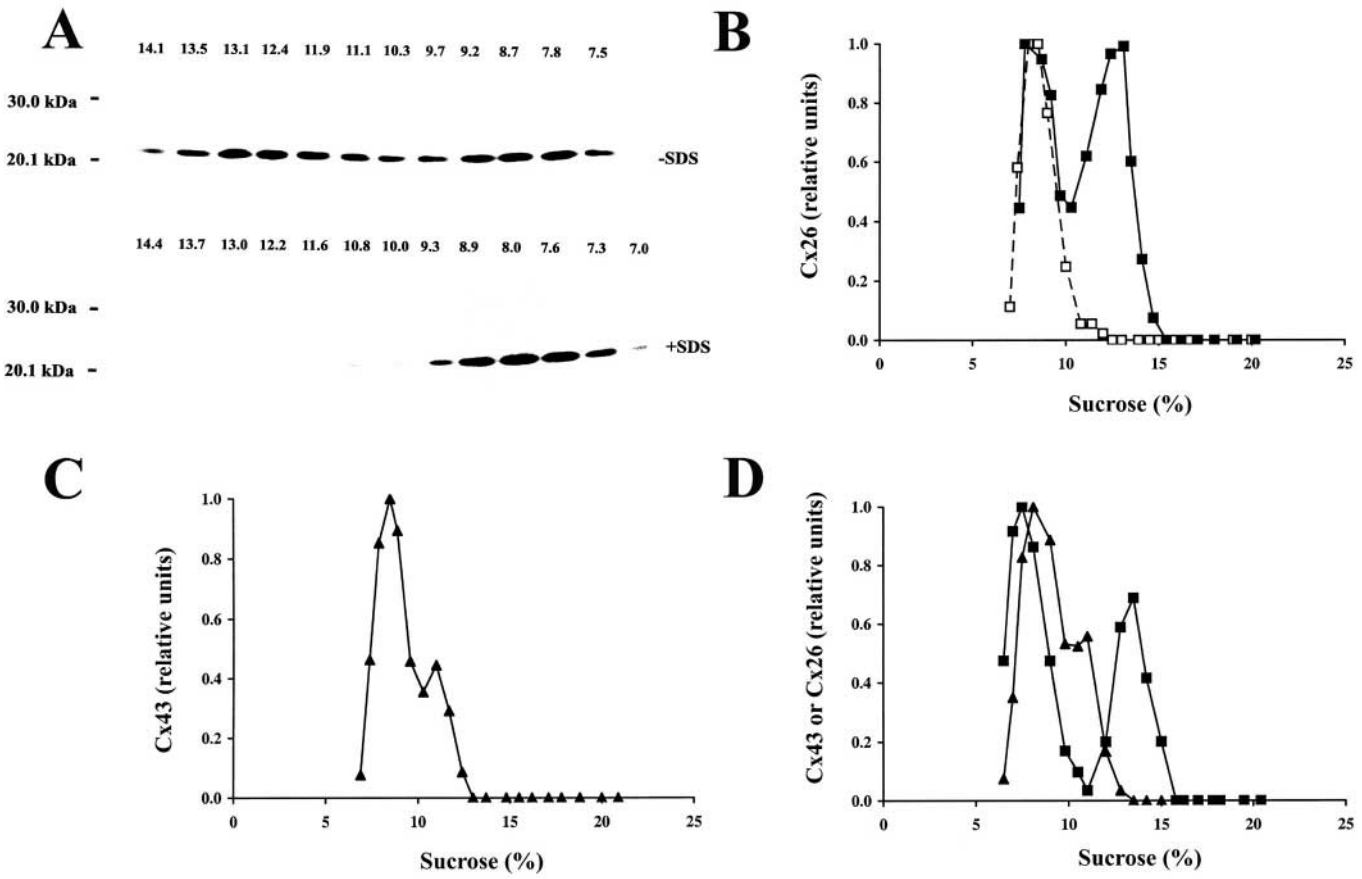


**Fig. 7.** Analysis of oligomeric association of Cx26 and/or Cx43 in Hela-Cx26 (A,B), HeLa-Cx43 (C), and HeLa-Cx43/Cx26 cells (D). (A) Immunoblot of fractions collected after centrifugation of Triton X-100 soluble extract from Hela-Cx26 cells through a 5-20% sucrose gradient. Prior to centrifugation, samples were incubated in buffer alone (top panel) or buffer containing 0.6% SDS to disrupt oligomers (bottom panel). The numbers under the lanes indicate the corresponding sucrose concentration as determined by refractometry. (B-D) Graphs of the densitometric values obtained after quantitation of Cx43 (triangles) or Cx26 (open and solid squares) immunoblots. For HeLa-Cx26 cells, the Triton-soluble material was untreated (■) or treated (□) with 0.6% SDS for 1 hour at 4°C before layering on the top of the sucrose gradient.

(He et al., 1999; Valiunas et al., 2001) and between combinations of β-connexins including Cx32 and Cx26 (Bevans et al., 1998) and Cx26 and Cx30 (Ahmad et al., 2003). Our data showing incompatibility of Cx26 and Cx43 are consistent with a lack of interactions between members of the two groups. Previous experiments have suggested that Cx43 (α) and Cx32 (β) are also incompatible (Guerrier et al., 1995; Falk et al., 1997; Das Sarma et al., 2001). How the classification scheme will explain the compatibility or incompatibility of more distant connexin sequences (that may be members of other subgroups) like Cx45 or Cx36 is not clear. Clearly, Cx45 can form functional heterotypic (Elenes et al., 2001) and heteromeric (Martinez et al., 2002) combinations with Cx43.

What are the mechanisms that allow or restrict hetero-oligomerization of connexins? Connexins might be prevented from mixing through formation of connexons at different cellular sites. The best cases for this mechanism might be Cx32 and Cx43 which oligomerize in the endoplasmic reticulum and Golgi apparatus, respectively (Musil and Goodenough, 1993; Das Sarma et al., 2001). Evans and colleagues have proposed

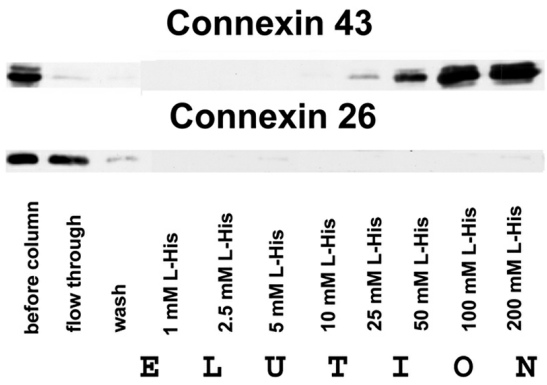


**Fig. 8.** Affinity purification of Cx43 and potential associated proteins from N2a-Cx43(His)$_6$/Cx26 cells. A Triton X-100-soluble extract was purified using a Ni-NTA resin and eluted with a series of increasing concentrations of L-histidine (as indicated). The presence and abundance of Cx43 and Cx26 were analyzed by immunoblotting in the cell extract, washes and eluted material using anti-Cx43 and anti-Cx26 antibodies.

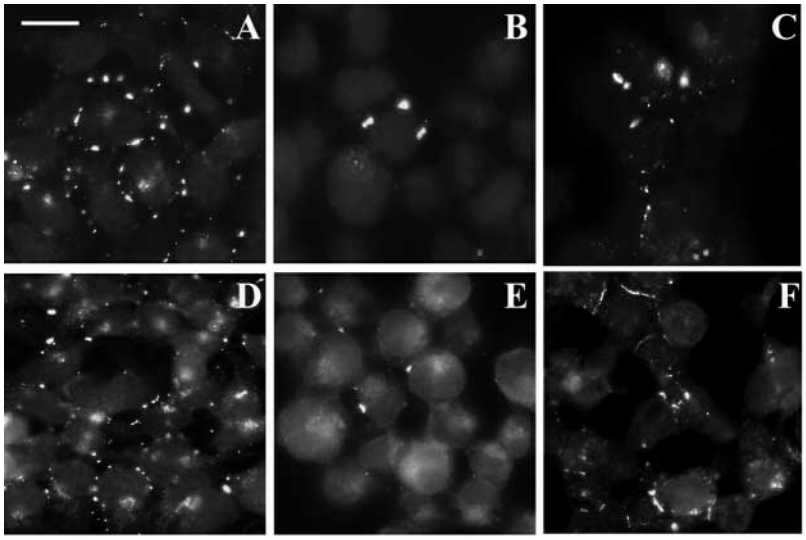


**Fig. 9.** Effects of brefeldin A or nocodazole (20 hour treatment) on the distribution of Cx26 and Cx43 in HEK- Cx26 cells. Immunofluorescent images of cells labeled for Cx26 (A-C) and for Cx43 (D-F). (A,D) Control cells; (B,E) cells treated with brefeldin A; (C,F) cells treated with nocodazole. Bar: 20 μm.

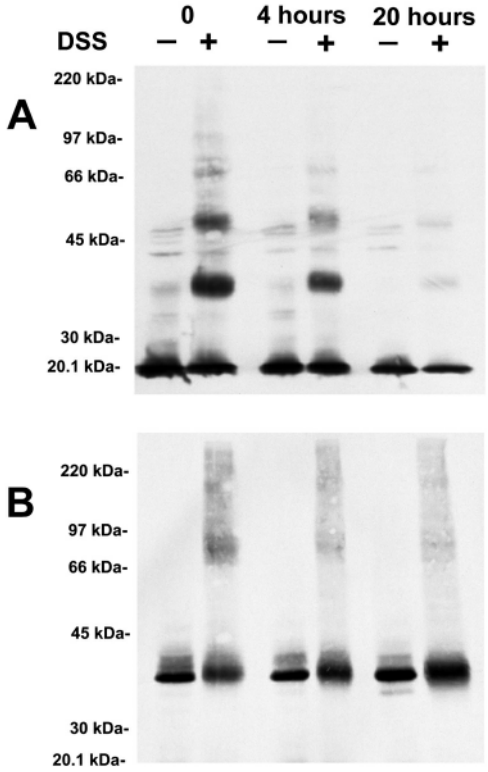


**Fig. 10.** Cross-linking of connexins in HeLa-Cx43/Cx26 cells untreated or treated with brefeldin A for 4 hours or 20 hours. Triton X-100 soluble extracts (containing connexons) were reacted with disuccinimyl suberate (DSS) cross-linker dissolved in DMSO (+) or were incubated with DMSO solvent alone (–). Samples containing 100 μg protein were resolved by SDS-PAGE, and Cx26 (A) or Cx43 (B) were detected by immunoblot analysis using anti-Cx26 or anti-Cx43 antibodies. Migration of molecular mass markers is indicated to the left of the blot.

that Cx26 follows an alternative pathway for cellular trafficking (Evans et al., 1999; Martin et al., 2001); this might prevent its exposure to other connexins. However, when co-expressed with Cx32, Cx26 is found together with Cx32 in some cellular compartments, and they form heteromeric connexons (Diez et al., 1999; Ahmad et al., 1999). Moreover, our own pharmacologic studies involving treatment of co-expressing cells with brefeldin A or nocodazole suggested that both Cx26 and Cx43 followed similar routes of cellular trafficking and assembly into gap junctions in our HEK and HeLa cells. Recently, Lagree et al. (Lagree et al., 2003) examined the incompatibility of Cx32 and Cx43 to begin to define molecular determinants of connexin mixing; their dye transfer and immunolocalization studies of site-directed mutants suggest that residues in the N-terminus (positions 12 and 13 of Cx43) and transmembrane domain 3 were important for oligomerization.

Although Cx26 and Cx43 did not form heteromeric channels, the co-expression of these two connexins was not without consequences. Co-expression of Cx26 and Cx43 reduced the total junctional conductance to a little more than 10% of that in cells expressing only a single connexin (Table 1). A reduction of almost the same magnitude was observed when co-expressing cells were paired with N2aCx26 or N2aCx43 cells. This decrease cannot be explained by the formation of non-functional heteromers (since heteromers could not be detected biochemically) which may explain the reduced conductance in cells co-expressing Cx40 and Cx43 (Valiunas et al., 2001). Moreover, the decrease is probably not due to non-functional heterotypic pairings of Cx26 and Cx43, since these cells contained large domains that primarily contained only a single connexin.

However, it does seem that the presence of the two incompatible connexins in the same plaques prevented the cells from achieving a comparable level of coupling as when case when all connexins are compatible. Bukauskas et al., (Bukauskas et al., 2001) have recently used quantitation of junctional channels in cells expressing a GFP-tagged connexin to demonstrate that a large number of channels within a plaque are non-functional. It appears that an interfering interaction occurred when Cx26 and Cx43 were co-expressed that led to an even smaller number of functioning channels. The presence of incompatible connexons might have substantially reduced the level of functional docking.

It is also possible that the lowered conductance represents a case where adjacent channels composed of Cx26 and Cx43 do not display cooperative gating behavior (or actually interfere with the cooperative behavior of each other) reducing the total number of conducting channels at any one instance in time and hence lowering macroscopic junctional conductance. The examples of cooperative gating in the literature manifest themselves as non-Poisson distributions and are most easily illustrated by phenomena such as one channel of two having an open probability of 90% while the other is at 10%, over intervals of time that exclude too short a sampling time as an explanation (Manivannan et al., 1992; Brink et al., 1996; Srinivas et al., 1999). Assuming the co-expression effect to be one associated with cooperative gating processes leads to the following possible explanation: interactions between connexons might trigger prolonged channel silencing where channels close for many minutes at a time; the Cx26 channels (by close association in the membrane with Cx43 connexons) would affect the gating of Cx43 channels (and vice versa). Unfortunately, we do not have adequate long recordings with few channels from the co-expressing cells to obtain unequivocal data regarding this possibility.

The reduced conductance appears to apply only to co-expression of Cx26 and Cx43 in mammalian cells, since they produced an additive increase when co-expressed in *Xenopus* oocytes (Rouan et al., 2001). We can only explain this difference between results as due to the different characteristics of the *Xenopus* oocyte pair and transfected cell expression systems. It is probable that the appositional regions of plasma membrane in small eukaryotic cells (like N2a cells) have only a limited capacity for connexons (or total gap junction plaque size). If that ceiling were reached in stably transfected cells with the introduced connexin robustly expressed from a viral promoter, addition of a second (incompatible) connexin would actually decrease the abundance of functional channels within the contacting membranes. In contrast, the capacity for expression of gap junction channels by the *Xenopus* oocytes is much greater. If that capacity had not been reached, injection of a second connexin RNA would lead to increased numbers of junctional channels in the plasma membrane and increased conductance (approximating the sum of the conductances produced by the RNAs for the two incompatible connexins).

Regardless of its explanation, our results imply that even co-expression of 'incompatible' connexins may dramatically alter the magnitude of intercellular communication between cells.

Bogdan Goc provided valuable technical assistance. This work was supported by NIH grants HL45466 and HL59199 and the Bernice Meltzer Pediatric Cancer Research Fund.

## References

**Ahmad, S., Chen, S., Sun, J. and Lin, X.** (2003). Connexins 26 and 30 are co-assembled to form gap junctions in the cochlea of mice. *Biochem. Biophys. Res. Commun.* **307**, 362-368.

**Ahmad, S., Diez, J. A., George, C. H. and Evans, W. H.** (1999). Synthesis and assembly of connexins in vitro into homomeric and heteromeric functional gap junction hemichannels. *Biochem. J.* **339**, 247-253.

**Barrio, L. C., Suchyna, T., Bargiello, T., Xu, L. X., Roginski, R. S., Bennett, M. V. and Nicholson, B. J.** (1991). Gap junctions formed by connexins 26 and 32 alone and in combination are differently affected by applied voltage. *Proc. Natl. Acad. Sci. USA* **88**, 8410-8414.

**Belliveau, D. J., Bechberger, J. F., Rogers, K. A. and Naus, C. C.** (1997). Differential expression of gap junctions in neurons and astrocytes derived from P19 embryonal carcinoma cells. *Dev. Genet.* **21**, 187-200.

**Berthoud, V. M., Montegna, E. A., Atal, N., Aithal, N. H., Brink, P. R. and Beyer, E. C.** (2001). Heteromeric connexons formed by the lens connexins, connexin43 and connexin56. *Eur. J. Cell Biol.* **80**, 11-19.

**Bevans, C. G., Kordel, M., Rhee, S. K. and Harris, A. L.** (1998). Isoform composition of connexin channels determines selectivity among second messengers and uncharged molecules. *J. Biol. Chem.* **273**, 2808-2816.

**Bradford, M. M.** (1976). A rapid and sensitive method for the quantitation of microgram quantities of protein using the principle of protein-dye binding. *Anal. Biochem.* **72**, 248-254.

**Brehm, R., Marks, A., Rey, R., Kliesch, S., Bergmann, M. and Steger, K.** (2002). Altered expression of connexins 26 and 43 in Sertoli cells in seminiferous tubules infiltrated with carcinoma-in-situ or seminoma. *J. Pathol.* **197**, 647-653.

**Brink, P. R., Cronin, K., Banach, K., Peterson, E., Westphale, E. M., Seul, K. H., Ramanan, S. V. and Beyer, E. C.** (1997). Evidence for heteromeric gap junction channels formed from rat connexin43 and human connexin37. *Am. J. Physiol. (Cell Physiol.)* **273**, C1386-C1396.

**Brink, P. R., Ramanan, S. V. and Christ, G. J.** (1996). Human connexin 43 gap junction channel gating: evidence for mode shifts and/or heterogeneity. *Am. J. Physiol.* **271**, C321-C331.

**Bukauskas, F. F., Bukauskiene, A., Bennett, M. V. and Verselis, V. K.** (2001). Gating properties of gap junction channels assembled from connexin43 and connexin43 fused with green fluorescent protein. *Biophys. J* **81**, 137-152.

**Charles, A. C., Kodali, S. K. and Tyndale, R. F.** (1996). Intercellular calcium waves in neurons. *Mol. Cell Neurosci.* **7**, 337-353.

**Das Sarma, J., Meyer, R. A., Wang, F., Abraham, V., Lo, C. W. and Koval, M.** (2001). Multimeric connexin interactions prior to the trans-Golgi network. *J. Cell Sci.* **114**, 4013-4024.

**Diez, J. A., Ahmad, S. and Evans, W. H.** (1999). Assembly of heteromeric connexons in guinea-pig liver en route to the Golgi apparatus, plasma membrane and gap junctions. *Eur. J. Biochem.* **262**, 142-148.

**Elenes, S., Martinez, A. D., Delmar, M., Beyer, E. C. and Moreno, A. P.** (2001). Heterotypic docking of Cx43 and Cx45 connexons blocks fast voltage gating of Cx43. *Biophys. J.* **81**, 1406-1418.

**Elfgang, C., Eckert, R., Lichtenberg-Frate, H., Butterweck, A., Traub, O., Klein, R. A., Hulser, D. F. and Willecke, K.** (1995). Specific permeability and selective formation of gap junction channels in connexin-transfected HeLa cells. *J. Cell Biol.* **129**, 805-817.

**Evans, W. H., Ahmad, S., Diez, J., George, C. H., Kendall, J. M. and Martin, P. E.** (1999). Trafficking pathways leading to the formation of gap junctions. *Novartis. Found. Symp.* **219**, 44-54.

**Falk, M. M.** (2000). Connexin-specific distribution within gap junctions revealed in living cells. *J. Cell Sci.* **113**, 4109-4120.

**Falk, M. M., Buehler, L. K., Kumar, N. M. and Gilula, N. B.** (1997). Cell-free synthesis and assembly of connexins into functional gap junction membrane channels. *EMBO J.* **16**, 2703-2716.

**Fishman, P. H. and Curran, P. K.** (1992). Brefeldin A inhibits protein synthesis in cultured cells. *FEBS Lett.* **314**, 371-374.

**George, C. H., Kendall, J. M. and Evans, W. H.** (1999). Intracellular trafficking pathways in the assembly of connexins into gap junctions. *J. Biol. Chem.* **274**, 8678-8685.

**Goliger, J. A. and Paul, D. L.** (1995). Wounding alters epidermal connexin expression and gap junction-mediated intercellular communication. *Mol. Biol. Cell* **6**, 1491-1501.

**Guerrier, A., Fonlupt, P., Morand, I., Rabilloud, R., Audebet, C., Krutovskikh, V., Gros, D., Rousset, B. and Munari-Silem, Y.** (1995). Gap junctions and cell polarity: connexin32 and connexin43 expressed in polarized thyroid epithelial cells assemble into separate gap junctions, which are located in distinct regions of the lateral plasma membrane domain. *J. Cell Sci.* **108**, 2609-2617.

**Harris, A. L.** (2001). Emerging issues of connexin channels: biophysics fills the gap. *Q. Rev. Biophys.* **34**, 325-472.

**He, D. S., Jiang, J. X., Taffet, S. M. and Burt, J. M.** (1999). Formation of heteromeric gap junction channels by connexins 40 and 43 in vascular smooth muscle cells. *Proc. Natl. Acad. Sci. USA* **96**, 6495-6500.

**Hunter, A. W., Jourdan, J. and Gourdie, R. G.** (2003). Fusion of GFP to the Carboxyl Terminus of Connexin43 Increases Gap Junction Size in HeLa Cells. *Cell Commun. Adhes.* **10**, 211-214.

**Jiang, J. X. and Goodenough, D. A.** (1996). Heteromeric connexons in lens gap junction channels. *Proc. Natl. Acad. Sci. USA* **93**, 1287-1291.

**Johnson, R. G., Meyer, R. A., Li, X. R., Preus, D. M., Tan, L., Grunenwald,**

**H., Paulson, A. F., Laird, D. W. and Sheridan, J. D.** (2002). Gap junctions assemble in the presence of cytoskeletal inhibitors, but enhanced assembly requires microtubules. *Exp. Cell Res.* **275**, 67-80.

**Kanter, H. L., Laing, J. G., Beau, S. L., Beyer, E. C. and Saffitz, J. E.** (1993). Distinct patterns of connexin expression in canine Purkinje fibers and ventricular muscle. *Circ. Res.* **72**, 1124-1131.

**Kikuchi, T., Kimura, R. S., Paul, D. L., Takasaka, T. and Adams, J. C.** (2000). Gap junction systems in the mammalian cochlea. *Brain Res. Brain Res. Rev.* **32**, 163-166.

**Koval, M., Harley, J. E., Hick, E. and Steinberg, T. H.** (1997). Connexin46 is retained as monomers in a trans-Golgi compartment of osteoblastic cells. *J. Cell Biol.* **137**, 847-857.

**Krisciukaitis, A.** (1997). Computer programs for investigation of intercellular communication using double whole-cell voltage clamp. *Electron. Electric. Eng.* **4**, 71-83.

**Kumar, N. M.** (1999). Molecular biology of the interactions between connexins. *Novartis. Found. Symp.* **219**, 6-16.

**Kumar, N. M. and Gilula, N. B.** (1992). Molecular biology and genetics of gap junction channels. *Semin. Cell Biol.* **3**, 3-16.

**Lagree, V., Brunschwig, K., Lopez, P., Gilula, N. B., Richard, G. and Falk, M. M.** (2003). Specific amino-acid residues in the N-terminus and TM3 implicated in channel function and oligomerization compatibility of connexin43. *J. Cell Sci.* **116**, 3189-3201.

**Laing, J. G. and Beyer, E. C.** (1995). The gap junction protein connexin43 is degraded via the ubiquitin proteasome pathway. *J. Biol. Chem.* **270**, 26399-26403.

**Lee, Y. C., Yellowley, C. E., Li, Z., Donahue, H. J. and Rannels, D. E.** (1997). Expression of functional gap junctions in cultured pulmonary alveolar epithelial cells. *Am. J. Physiol.* **272**, L1105-L1114.

**Manivannan, K., Ramanan, S. V., Mathias, R. T. and Brink, P. R.** (1992). Multichannel recordings from membranes which contain gap junctions. *Biophys. J.* **61**, 216-227.

**Martin, P. E., Blundell, G., Ahmad, S., Errington, R. J. and Evans, W. H.** (2001). Multiple pathways in the trafficking and assembly of connexin 26, 32 and 43 into gap junction intercellular communication channels. *J. Cell Sci.* **114**, 3845-3855.

**Martinez, A. D., Hayrapetyan, V., Moreno, A. P. and Beyer, E. C.** (2002). Connexin43 and connexin45 form heteromeric gap junction channels in which individual components determine permeability and regulation. *Circ. Res.* **90**, 1100-1107.

**Meda, P., Pepper, M. S., Traub, O., Willecke, K., Gros, D., Beyer, E., Nicholson, B., Paul, D. and Orci, L.** (1993). Differential expression of gap junction connexins in endocrine and exocrine glands. *Endocrinology* **133**, 2371-2378.

**Musil, L. S. and Goodenough, D. A.** (1993). Multisubunit assembly of an integral plasma membrane channel protein, gap junction connexin43, occurs after exit from the ER. *Cell* **74**, 1065-1077.

**Nagy, J. I., Li, X., Rempel, J., Stelmack, G., Patel, D., Staines, W. A., Yasumura, T. and Rash, J. E.** (2001). Connexin26 in adult rodent central nervous system: demonstration at astrocytic gap junctions and colocalization with connexin30 and connexin43. *J. Comp. Neurol.* **441**, 302-323.

**Ramanan, S. V., Brink, P. R., Varadaraj, K., Peterson, E., Schirrmacher, K. and Banach, K.** (1999). A three-state model for connexin37 gating kinetics. *Biophys. J.* **76**, 2520-2529.

**Risek, B., Klier, F. G. and Gilula, N. B.** (1994). Developmental regulation and structural organization of connexins in epidermal gap junctions. *Dev. Biol.* **164**, 183-196.

**Rouan, F., White, T. W., Brown, N., Taylor, A. M., Lucke, T. W., Paul, D. L., Munro, C. S., Uitto, J., Hodgins, M. B. and Richard, G.** (2001). Trans-dominant inhibition of connexin-43 by mutant connexin-26: implications for dominant connexin disorders affecting epidermal differentiation. *J. Cell Sci.* **114**, 2105-2113.

**Spray, D. C., Moreno, A. P., Kessler, J. A. and Dermietzel, R.** (1991). Characterization of gap junctions between cultured leptomeningeal cells. *Brain Res.* **568**, 1-14.

**Srinivas, M., Costa, M., Gao, Y., Fort, A., Fishman, G. I. and Spray, D. C.** (1999). Voltage dependence of macroscopic and unitary currents of gap junction channels formed by mouse connexin50 expressed in rat neuroblastoma cells. *J. Physiol.* **517**, 673-689.

**Stauffer, K. A.** (1995). The gap junction proteins beta(1)-connexin (connexin-32) and beta(2)-connexin (connexin-26) can form heteromeric hemichannels. *J. Biol. Chem.* **270**, 6768-6772.

**Suchyna, T. M., Nitsche, J. M., Chilton, M., Harris, A. L., Veenstra, R. D. and Nicholson, B. J.** (1999). Different ionic selectivities for connexins 26 and 32 produce rectifying gap junction channels. *Biophys. J.* **77**, 2968-2987.

**Swenson, K. I., Jordan, J. R., Beyer, E. C. and Paul, D. L.** (1989). Formation of gap junctions by expression of connexins in Xenopus oocyte pairs. *Cell* **57**, 145-155.

**Thomas, T., Jordan, K. and Laird, D. W.** (2001). Role of cytoskeletal elements in the recruitment of Cx43-GFP and Cx26-YFP into gap junctions. *Cell Commun. Adhes.* **8**, 231-236.

**Tomasetto, C., Neveu, M. J., Daley, J., Horan, P. K. and Sager, R.** (1993). Specificity of gap junction communication among human mammary cells and connexin transfectants in culture. *J. Cell Biol.* **122**, 157-167.

**Valiunas, V., Weingart, R. and Brink, P. R.** (2000). Formation of heterotypic gap junction channels by connexins 40 and 43. *Circ. Res.* **86**, E42-E49.

**Valiunas, V., Gemel, J., Brink, P. R. and Beyer, E. C.** (2001). Gap junction channels formed by coexpressed connexin40 and connexin43. *Am. J. Physiol. (Heart Circ. Physiol.)* **281**, H1675-H1689.

**Veenstra, R. D., Wang, H. Z., Westphale, E. M. and Beyer, E. C.** (1992). Multiple connexins confer distinct regulatory and conductance properties of gap junctions in developing heart. *Circ. Res.* **71**, 1277-1283.

**Verselis, V. K., Bargiello, T. A., Rubin, J. A. and Bennett, M. V. L.** (1993). Comparison of voltage dependent properties of gap junctions in hepatocytes and in Xenopus oocytes expressing Cx32 and Cx26. *Prog. Cell Res.* **3**, 105-112.

**Verselis, V. K., Bennett, M. V. L. and Bargiello, T. A.** (1991). A voltage-dependent gap junction in Drosophila melanogaster. *Biophys. J.* **59**, 114-125.

**Werner, R., Levine, E., Rabadan Diehl, C. and Dahl, G.** (1989). Formation of hybrid cell-cell channels. *Proc. Natl. Acad. Sci. USA* **86**, 5380-5384.

**White, T. W. and Bruzzone, R.** (1996). Multiple connexin proteins in single intercellular channels: connexin compatibility and functional consequences. *J. Bioenerg. Biomembr.* **28**, 339-350.

**White, T. W., Paul, D. L., Goodenough, D. A. and Bruzzone, R.** (1995). Functional analysis of selective interactions among rodent connexins. *Mol. Biol. Cell* **6**, 459-470.

**Willecke, K., Eiberger, J., Degen, J., Eckardt, D., Romualdi, A., Guldenagel, M., Deutsch, U. and Sohl, G.** (2002). Structural and functional diversity of connexin genes in the mouse and human genome. *Biol. Chem.* **383**, 725-737.

**Yeager, M. and Nicholson, B. J.** (1996). Structure of gap junction intercellular channels. *Curr. Opin. Struct. Biol.* **6**, 183-192.